Mechanism of N-WASP Activation by CDC42 and Phosphatidylinositol 4,5-bisphosphate

Rajat Rohatgi, Hsin-yi Henry Ho, and Marc W. Kirschner

Department of Cell Biology, Harvard Medical School, Boston, Massachusetts 02115

Abstract. Neuronal Wiskott-Aldrich Syndrome protein (N-WASP) transmits signals from Cdc42 to the nucleation of actin filaments by Arp2/3 complex. Although full-length N-WASP is a weak activator of Arp2/3 complex, its activity can be enhanced by upstream regulators such as Cdc42 and $PI(4,5)P_2$. We dissected this activation reaction and found that the previously described physical interaction between the NH_2-terminal domain and the COOH-terminal effector domain of N-WASP is a regulatory interaction because it can inhibit the actin nucleation activity of the effector domain by occluding the Arp2/3 binding site. This interaction between the NH_2- and COOH termini must be intramolecular because in solution N-WASP is a monomer. Phosphatidylinositol 4,5-bisphosphate ($PI(4,5)P_2$) influences the activity of N-WASP through a conserved basic sequence element located near the Cdc42 binding site rather than through the WASp homology domain 1. Like Cdc42, $PI(4,5)P_2$ reduces the affinity between the NH_2- and COOH termini of the molecule. The use of a mutant N-WASP molecule lacking this basic stretch allowed us to delineate a signaling pathway in *Xenopus* extracts leading from $PI(4,5)P_2$ to actin nucleation through Cdc42, N-WASP, and Arp2/3 complex. In this pathway, $PI(4,5)P_2$ serves two functions: first, as an activator of N-WASP; and second, as an indirect activator of Cdc42.

Key words: phosphoinositides • Cdc42 GTP-binding protein • actin • signal transduction • Wiskott-Aldrich Syndrome protein

Introduction

The Rho family of small GTPases can direct distinct morphological changes in the actin cytoskeleton. The three founding members of the Rho family, Rho, Rac, and Cdc42, induce the formation of stress fibers, lamellipodia, and filopodia when introduced into cells (Hall, 1998). Whereas Rho functions by reorganizing preexisting actin filaments, Rac and Cdc42 act by promoting new actin polymerization, either by stimulating de novo actin nucleation or by stimulating the uncapping or severing of filaments (Machesky and Insall, 1999). Over the last two years, proteins of the Wiskott Aldrich Syndrome protein (WASp)[1] family have emerged as important mediators of the de novo actin nucleation pathway downstream of Rac and Cdc42 (Mullins, 2000). The first member of this family, WASp, was identified as a gene expressed in the hematopoietic lineage that is mutated in children with the disease Wiskott Aldrich Syndrome (Derry et al., 1994). Other family members include neuronal WASp (N-WASP), a ubiquitously expressed protein with ~50% identity to WASp, Bee1/Las17p from yeast, and the Scar/WAVE proteins (Miki et al., 1996, 1998b; Li, 1997; Bear et al., 1998; Suetsugu et al., 1999).

The WASp family proteins funnel signals from a variety of upstream signaling pathways to actin nucleation through a common effector, Arp2/3 complex. For instance, N-WASP has been implicated in filopodia formation downstream of Cdc42, and the Scar/WAVE family has been shown to function in lamellipodia formation downstream of Rac in fibroblasts and in actin polymerization downstream of the cAMP receptor in *Dictyostelium* (Bear et al., 1998; Miki et al., 1998a,b). In turn, Arp2/3 complex can accelerate the de novo nucleation of actin filaments and can also orga-

R. Rohatgi and H.H. Ho contributed equally to this study.

Address correspondence to Marc Kirschner, Department of Cell Biology, Harvard Medical School, 240 Longwood Avenue, Boston, MA 02115. Tel.: (617) 432-2250. Fax: (617) 432-0420. E-mail: marc@hms.harvard.edu

[1]*Abbreviations used in this paper:* A, acidic region; BR, basic region; C, cofilin homology segment; CRIB, Cdc42/Rac interactive motif; G-actin, actin monomers; GBD, G-protein binding domain; G-protein, GTP binding protein; GBR, G-protein binding region; GST, glutathione S-transferase; HT, hexahistidine-tagged; HSS, high speed supernatant; MT, Myc-tagged; NMR, nuclear magnetic resonance; N-WASP, neuronal WASP; PC, phosphatidylcholine; PI, phosphatidylinositol; $PI(4,5)P_2$, PI 4,5-bisphosphate; PRD, proline-rich domain; V, verprolin homology segment; VCA, COOH-terminal domain of WASP family proteins containing the V, C, and A segments; WASp, Wiskott-Aldrich Syndrome protein; WH1, WASp homology domain 1; WIP, WASp interacting protein.

nize these filaments into the stereotypical arrays seen at the leading edges of migrating cells (Mullins et al., 1998; Svitkina and Borisy, 1999). This property of different upstream targets and a common downstream effector is reflected in the domain structure of WASp family proteins. They contain a conserved COOH-terminal VCA domain, consisting of a verprolin homology segment (V), a cofilin homology segment (C) and an acidic region (A) (see Fig. 1 A; Miki et al., 1996). The VCA domains of various family members have been the focus of extensive investigation because these domains of ~100 residues can bind actin monomers (G-actin) and Arp2/3 complex, interactions that lead to a dramatic enhancement of actin nucleation by Arp2/3 complex (Egile et al., 1999; Machesky et al., 1999; Rohatgi et al., 1999; Winter et al., 1999; Yarar et al., 1999).

On the other hand, the NH_2 termini of WASp family proteins are quite diverse and, therefore, are thought to interact with distinct sets of upstream signaling molecules. In particular, the NH_2 termini of N-WASP and WASp contain several recognizable and biochemically defined domains (see Fig. 1 A). The extreme NH_2 termini of WASp and N-WASP contain a WASp homology 1 (WH1) domain that mediates interactions with the WASp interacting protein (WIP) family, calmodulin, $PI(4,5)P_2$, and actin filaments (Miki et al., 1996; Ramesh et al., 1997; Egile et al., 1999). The WH1 domain is followed by a Cdc42 or G-protein binding domain (GBD), which includes a Cdc42/Rac interactive binding (CRIB) motif (Aspenstrom et al., 1996; Kolluri et al., 1996; Symons et al., 1996; Miki et al., 1998a). In all WASp family members, the NH_2-terminal domains are linked to the COOH-terminal VCA segment through a long proline-rich region, which is implicated in binding to profilin and to Src homology domain 3–containing proteins like Grb2, Nck, and certain cytoplasmic tyrosine kinases (Rivero-Lezcano et al., 1995; Banin et al., 1996; Miki et al., 1996; She et al., 1997). Given this remarkable list of interacting partners, the WASp family of proteins, endowed with multiple domains for interactions with a large number of other signaling molecules, appear to be ideally built for integrating diverse upstream signals and relaying them to Arp2/3 complex. Thus, a detailed biochemical understanding of how WASp family proteins are activated (and subsequently inactivated) is crucial for understanding how signaling pathways attain precise spatial and temporal control over actin polymerization in the cell.

N-WASP is the only WASp family member whose biochemical activity towards Arp2/3 complex has been shown to be directly enhanced by upstream signaling molecules, including Cdc42, $PI(4,5)P_2$, Grb2, and the *Shigella* protein IcsA (Egile et al., 1999; Rohatgi et al., 1999; Carlier et al., 2000). We have reconstituted one minimal scheme for the signal-regulated activation of N-WASP using purified components in vitro. Full-length N-WASP, which displays weak basal activity towards Arp2/3 complex, can be dramatically and synergistically activated by Cdc42 and $PI(4,5)P_2$. This behavior of full-length N-WASP can be accounted for by an allosteric model for N-WASP regulation. Miki et al. (1998a) first demonstrated that activated Cdc42 and N-WASP can cooperate to induce filopodia when introduced into tissue culture cells. In exploring the regulation of N-WASP by Cdc42, they found that a fragment of N-WASP containing the GBD could physically interact with the COOH-terminal VCA segment, and this interaction could be relieved by the binding of Cdc42 to the GBD domain (Miki et al., 1998a). These data suggested the following: that N-WASP exists in a closed, autoinhibited state; and that binding of activated Cdc42 to the GBD would release intramolecular contacts in the molecule, unmasking the VCA region. A recently published nuclear magnetic resonance (NMR) study of WASp provided a detailed structural model for the interaction between NH_2-terminal GBD and the VCA segment (Kim et al., 2000). Using an engineered WASp construct in which the GBD domain was fused via a short linker to a fragment from the COOH-terminal cofilin-acidic (CA) segment, the authors demonstrated that the GBD domain of WASp folds into markedly different and mutually incompatible structures depending upon whether it is bound to Cdc42 or to the CA fragment.

From the standpoint of N-WASP activation, the critical question about this physical interaction between the NH_2- and COOH-terminal domains of N-WASP remains to be answered. Does this interaction regulate the activity of N-WASP by inhibiting the activity of the VCA segment? Since binding of the VCA segment to both G-actin and Arp2/3 is required for stimulation of nucleation, does this interaction inhibit nucleation by occluding the Arp2/3 binding site, the G-actin binding site, or both? Whereas the interactions between Cdc42 and N-WASP have been examined, the biochemical mechanism by which $PI(4,5)P_2$ activates N-WASP as well as the sequence elements in N-WASP necessary to respond to $PI(4,5)P_2$ remain obscure. In this study, we have taken advantage of the remarkably parsimonious and biochemically reconstituted Cdc42-$PI(4,5)P_2$-N-WASP-Arp2/3 signaling module to answer these questions and to test the current models for how N-WASP is activated by Cdc42 and $PI(4,5)P_2$. This activation reaction will hopefully shed light on the regulation of WASp family members in general.

Materials and Methods

Antibodies

Arp2/3 complex was detected using a polyclonal antiserum against Arp2 or by using affinity-purified anti-Arp3 or anti-ARC34 antibodies provided by M. Welch (University of California, Berkeley, Berkeley, CA). The affinity-purified anti–N-WASP antibody has been described previously (Rohatgi et al., 1999). The anti-pentaHis (QIAGEN), anti-GST (Amersham Pharmacia Biotech), anti-Cdc42 (Santa Cruz Biotechnology, Inc.), and the antiactin (Amersham Pharmacia Biotech) antibodies were purchased.

Protein Expression and Purification

All N-WASP fragments and mutants were made by PCR using bovine N-WASP cDNA as the template and were confirmed by sequencing. The wild-type, full-length N-WASP used in this study (both GST-tagged and untagged) was the rat version.

To construct templates for in vitro translation, WGP (amino acids 1–396), WG (amino acids 1–277), WH1 (amino acids 1–158), and the G-protein binding region (GBR; amino acids 151–277) were subcloned into the pCS2 + MT vector containing six copies of the Myc epitope located NH_2-terminal to the cloning sites. The in vitro translation of ^{35}S-labeled proteins was performed using the TNT-coupled (transcription/translation) rabbit reticulocyte lysate system (Promega) and [^{35}S]methionine (NEN Life Science Products).

For production of recombinant proteins in Sf9 cells, baculoviruses were constructed and used for infections according to the Bac-to-Bac baculovirus expression system (GIBCO BRL). WGP and WG (without the Myc epitopes) were transferred from pCS2+ into the pFastBacHT vector (GIBCO BRL), which contains a hexahistidine tag located NH_2- terminal to the cloning sites. After expression, HT-WG and HT-WGP proteins were purified by Ni-NTA (QIAGEN) affinity chromatography. GST fusions of wild-type N-WASP, (ΔWH1)N-WASP (residues 151–505) and (ΔB)N-WASP (Δ residues 186–195) were generated by subcloning the inserts into a modified pFastBacHT vector carrying the sequence encoding GST inserted (in-frame) COOH-terminal to the hexahistidine tag and NH_2-terminal to the cloning sites. These proteins (tagged at their NH_2 termini with a hexahistidine tag followed by a GST tag) were purified on a Ni-NTA or glutathione Sepharose affinity column followed by a Mono Q column (Amersham Pharmacia Biotech).

For production of purified recombinant proteins in *Escherichia coli*, VCA (amino acids 392–505), VCA(Δcol)(Δ residues 477–480), V (amino acids 392–449), VC (amino acids 392–485), CA (amino acids 450–505), GBR (amino acids 151–277), GBR2 (amino acids 201–277), GBR3 (Δ residues 186–200), and GBR4 (with K186D, K189D, K192D, and K195D) were fused to GST at their NH_2 termini by cloning them into a pGEX vector (Amersham Pharmacia Biotech) and affinity-purified on glutathione Sepharose beads as described previously (Miki et al., 1996).

Purification of untagged full-length rat N-WASP (which was produced in Sf9 cells), Cdc42 (which was produced as a GST fusion and subsequently cleaved with thrombin to remove the GST tag), and Arp2/3 complex from bovine brain extracts has been described previously (Rohatgi et al., 1999). In the purified assay system, no difference was observed between prenylated (purified from Sf9 cell membranes) and nonprenylated (purified from *E. coli*) Cdc42. In some preparations of Arp2/3 complex, the Arp3 subunit appeared as a doublet (presumably because of partial proteolysis; see Fig. 2 c), an occurrence that did not affect the specific activity of the preparation either with respect to actin polymerization or VCA affinity.

Protein concentrations were determined by the Bradford assay (Bio-Rad Laboratories) or by scanning densitometry of Gelcode blue-stained gels (Pierce Chemical Co.) using BSA as a standard in both cases.

Hydrodynamic Measurements of Rat N-WASP

Analytical ultracentrifugation experiments were carried out at 4°C in 20 mM Hepes, pH 7.6, 100 mM KCl, 1 mM DTT in a Beckman Optima XL-A analytical ultracentrifuge. Sedimentation equilibrium experiments were performed at 20,000 rpm; sedimentation velocity experiments were performed at 40,000 rpm. Data collection and analysis were carried out using the Optima XL-A data analysis software and Microcal Origin. The partial specific volume of 0.713 cm^3/g for rat N-WASP was estimated from the amino acid content.

Gel filtration chromatography was performed on a Superdex 200 PC column (Amersham Phamacia Biotech) at 4°C using a Superdex200 column equilibrated in 20 mM Hepes, pH 7.6, 100 mM KCl, 1 mM DTT. To determine the diffusion coefficient (D) of rat N-WASP, standard curves were generated by plotting elution volume versus $1/D$, using the following protein standards (Amersham Pharmacia Biotech): ferritin, catalase, aldolase, BSA, and chymotrypsinogen A.

Binding Assays Using ^{35}S-labeled Proteins Produced in Reticulocyte Lysate

For GST pull-down assays, 5 μg of each GST fusion protein immobilized on 5 μl of glutathione-Sepharose beads was added to a 50-μl reaction containing XB buffer (20 mM Hepes, pH 7.7, 100 mM KCl, 1 mM $MgCl_2$, 0.1 mM EDTA), 1 mM DTT, 0.5 mg/ml chicken egg albumin as a carrier, and 10 μl of the [^{35}S]methionine-labeled target protein. After rotating at 4°C for 1 h, the beads were washed once with XB, 0.5 M KCl, 1 mM DTT, 0.1% Tween 20 (high salt wash), once with XB, 1 mM DTT, 0.5% Tween 20 (high detergent wash), and once with XB, 1 mM DTT, and 0.1% Tween 20 (low salt wash). Proteins bound to the beads were eluted with SDS sample buffer and analyzed by SDS-PAGE. The labeled proteins were visualized using a PhosphorImager (Bio-Rad Laboratories) and quantitated using Quantity One software (Bio-Rad Laboratories).

Binding Assays Using Purified Proteins

For Arp2/3 interaction assays, the GST-tagged protein (VCA, CA, or N-WASP) was incubated with the indicated concentrations of the other components (see Fig. 2) in 30 μl of XB plus 1 mM DTT, 0.02% Tween 20, 0.2 mM ATP, and 0.5 mg/ml chicken egg albumin (binding buffer). After a 1-h incubation in solution at room temperature, 5 μl of glutathione-Sepharose beads was added to each reaction and the GST-fused protein was captured by gently rocking this slurry at 4°C for an additional hour. The beads were collected by centrifugation and washed three times with 500 μl of XB plus 0.2 mM ATP, 1 mM DTT, and 0.02% Tween 20 (wash buffer). The proteins that remained bound to the beads were eluted with SDS sample buffer, fractionated by SDS-PAGE, and identified by immunoblotting. The G-actin binding assays were performed in the same manner, except that the binding and wash buffers contained 0.5× XB. To test the interaction of full-length, untagged N-WASP with Arp2/3 complex (see Fig. 2 e), 5 μl of glutathione-Sepharose beads coated with 5 μg of GST-Cdc42 were added to 40 μl of binding buffer containing Arp2/3 complex (1 μM) and the indicated concentrations of N-WASP and PI(4,5)P_2 vesicles.

Lipids

The preparation of synthetic liposomes used for pyrene actin assays has been described previously (Rohatgi et al., 1999). To make the [^{3}H]phosphatidylcholine-labeled vesicles used in lipid binding experiments, dried lipid mixtures (containing either PI(4,5)P_2 [30%] and PC [70%] or PI [30%] and PC [70%]) were resuspended in 30 mM Hepes, pH 7.0, 100 mM NaCl, 1 mM EDTA, and 0.02% NP-40 (HNE-NP-40) and sonicated to clarity. GST fusion proteins immobilized on glutathione-Sepharose beads (5 μg protein: 5 μl packed beads) were mixed with [^{3}H]phosphatidylcholine-labeled lipid vesicles (0.32 mM total lipid) in HNE-NP-40 in a total reaction volume of 50 μl. After a 1-h incubation with rotation at room temperature, the beads were collected by centrifugation, washed twice with HNE-NP-40 buffer, and subjected to liquid scintillation counting.

Xenopus Extracts and Immunodepletions

The preparation of high speed supernatant (HSS) from *Xenopus* egg extracts and the immunodepletion of N-WASP from these extracts have been described previously (Ma et al., 1998a; Rohatgi et al., 1999).

Actin Polymerization Assays

In *Xenopus* HSS, pyrene-labeled actin (2 μM) was added to follow actin polymerization as described previously (Ma et al., 1998a). After ensuring that the mixture achieved a stable baseline, polymerization was initiated by the addition of vesicles containing 10:45:45 PI(4,5)P_2/phosphatidylinositol (PI)/phosphatidylcholine (PC; 100 μM total lipid).

To follow actin polymerization using purified components, pyrene G-actin or unlabeled G-actin was isolated by incubating freshly thawed proteins in G buffer (5 mM Tris-HCl, pH 8.0, 0.2 mM $CaCl_2$, 0.2 mM ATP, 0.2 mM DTT) for ~10 h at 4°C, and then removing residual filamentous actin by centrifugation at 400,000 *g* for 1 h. Polymerization reactions contained 1.0 μM of unlabeled actin, 0.3 μM pyrene actin (50% labeled), and 0.2 mM ATP and various proteins at the indicated concentrations in 80 μl of XB buffer. All reaction components except actin were first mixed together in XB buffer. The reaction was started by adding a mixture of actin and pyrene actin, and the fluorescence changes were measured in a fluorometer. In all the curves shown in the figures, polymerization was initiated at time = 0; the curves are shifted along the abscissa to account for the delay time between the addition of actin and the first fluorescence reading.

Data Analysis

Kinetic analyses were performed using either the software provided with the fluorescence spectrometer (SLM-Aminco) or using MicroCal Origin. Maximum polymerization rates were calculated from the raw polymerization curves by performing a linear regression on the elongation phase of the actin assembly curve or by calculating the slope of the line tangent to the inflection point. In all the curves shown in the figures, solid lines are drawn through all the data points collected; a symbol is only placed on every few points for clarity. The data shown in the figures were taken from experiments performed at least two to three times. When normalized to controls, data varied by <20% between independent experiments.

Results

Association between the NH_2- and COOH-terminal Regions of N-WASP

The domain structure of the N-WASP molecule and its nomenclature is shown in Fig. 1 A. Unless otherwise noted, all residue numbers refer to the bovine N-WASP protein, which is ~95% identical to the human and rat versions. Since the domain nomenclature of WASp family proteins is not standardized, we begin with a brief description of the N-WASP domain structure and its designation used in this study (Fig. 1 A). The NH_2 terminus of the N-WASP molecule is composed of a WASP homology 1 (WH1) domain, followed by a GBR. The GBR contains a basic region (BR) and a GBD that interacts with Cdc42. The COOH terminus of N-WASP has been named a VCA segment because it contains two verprolin homology regions (V), a cofilin homology region (C), and an acidic region (A). The NH_2- and COOH-terminal portions of N-WASP are linked by a central proline-rich domain (PRD).

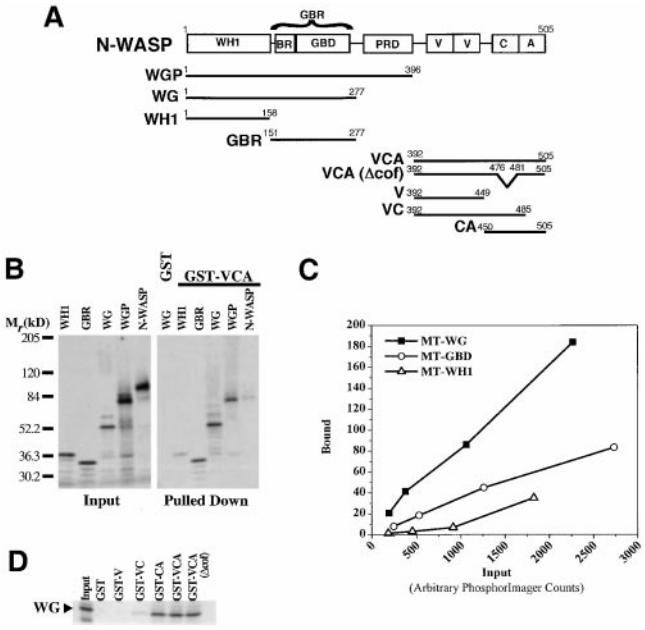

Figure 1. Sequence determinants of the interaction between the NH_2- and COOH-terminal regions of N-WASP. (A) A summary of the nomenclature and amino acid boundaries of the various domains and fragments of bovine N-WASP described in this study. (B) GST-VCA (or GST alone as a control) immobilized on glutathione-Sepharose beads was tested for its ability to pull down various fragments of N-WASP (shown in A) produced as Myc-tagged (MT), ^{35}S-labeled proteins. (C) Dose-dependent binding of the indicated N-WASP fragments to GST-VCA beads. The slope of the line defined by each set of points is inversely proportional to the dissociation constant. (D) GST fusions of the indicated subfragments of the VCA segment of N-WASP (defined in A) were immobilized on glutathione-Sepharose beads and used to pull down the MT-WG fragment from the NH_2 terminus of N-WASP. In B and D, 5% of the input and 33% of the pulled down material was analyzed on a 5–15% SDS–polyacrylamide gel.

The first evidence for the autoinhibited structure of N-WASP was the demonstration that the isolated VCA region could bind to an NH_2-terminal fragment (residues 127–277) that includes the GBR (Miki et al., 1998a). This interaction could be disrupted by the addition of Cdc42, suggesting that upstream activators might regulate N-WASP by reducing the affinity between the NH_2- and COOH termini. Since the NH_2- and COOH termini of N-WASP can interact even in the absence of the PRD that connects them in the full-length molecule, we wanted to determine whether the NH_2 terminus could inhibit, in trans, the ability of VCA to bind and activate Arp2/3 complex.

As a first step, we identified the portion of the NH_2 terminus of N-WASP that displayed the highest affinity for the VCA segment. Several N-WASP fragments were Myc-tagged (MT) at their NH_2 termini and were produced as [^{35}S]methionine-labeled proteins by in vitro translation (Fig. 1 A). The fragments have been named according to the domains of N-WASP that they encompass. For instance, MT-GBR is the Myc-tagged fragment that includes the GBR; MT-WG is the Myc-tagged fragment that includes the WH1 domain and the GBR; and MT-WGP is the Myc-tagged fragment that includes the WH1 domain, the GBR, and the PRD. These fragments were tested for their abilities to bind to a GST fusion of VCA (GST-VCA) using a pull-down assay. As expected, MT-WG, MT-WGP, and MT-GBR all bound to GST-VCA (Fig. 1 b). Surprisingly, a weak but detectable interaction was also observed between GST-VCA and the WH1 domain of N-WASP (Fig. 1, B and C). This additional VCA–WH1 interaction is one explanation for the observation that the MT-WG fragment bound to GST-VCA with an approximately twofold higher affinity than the MT-GBR fragment (Fig. 1 C). The full-length N-WASP molecule did not bind to GST-VCA, probably because its NH_2 terminus is locked in an intramolecular interaction with its COOH-terminal VCA segment and is, thus, unable to bind to GST-VCA added in trans (Fig. 1 B). The ^{35}S-labeled protein that bound to GST-VCA in the MT-N-WASP experiment is not full-length N-WASP, but rather a truncated translation product that does not include portions of the COOH-terminal VCA segment. In conclusion, the highest affinity for the VCA segment was seen with a fragment of N-WASP that included both the WH1 domain and GBR.

We also mapped the regions within VCA that are important for its interaction with the NH_2-terminal MT-WG fragment. Fragments containing the V, VC, CA, and VCA segments (Fig. 1 A) were expressed as GST fusion proteins and tested for their abilities to interact with the [^{35}S]methionine-labeled MT-WG fragment. The G-actin binding V segment appears to be dispensable for the interaction between VCA and MT-WG because GST-V does not bind to MT-WG and GST-CA and GST-VCA bind to MT-WG with roughly equal affinities (Fig. 1 D). The C segment contributes to the interaction since the GST-VC protein shows a weak interaction with MT-WG. However, the highest affinity interaction with MT-WG is seen when both the C and A segments are present (GST-CA and GST-VCA). This CA segment, which comprises the COOH-terminal 55 amino acids of N-WASP, is also the minimal region required for binding to Arp2/3 complex.

WASp family members have been postulated to interact

with Arp2/3 complex through a conserved 4–amino acid basic motif in the C segment (residues 477–480 [KRSK] in bovine N-WASP; Bi and Zigmond, 1999). In the recent NMR structure of the autoinhibited fold of human WASp, the first Arg in this motif makes a hydrogen bond to a glutamic acid residue in the GBD (Kim et al., 2000). Based on these results, the NH_2 termini of WASp family proteins may inhibit interactions between VCA and Arp2/3, at least in part, by occluding this motif. To test the hypothesis that this motif contributes to the affinity between VCA and the NH_2 terminus of N-WASP, we constructed a GST-VCA protein containing an in-frame deletion of these four residues (GST-VCA(Δcof; Fig. 1 A). The GST-VCA(Δcof) mutant bound to MT-WG as well as the wild-type VCA (Fig. 1 D). In addition, this mutation had only a very modest effect on the ability of GST-VCA to bind or to activate Arp2/3 complex (Rohatgi, R., and M.W. Kirschner, unpublished results).

The analysis presented above demonstrates that the GBR and the WH1 domains within the NH_2 terminus of N-WASP interact with the C and A segments in the COOH terminus of the molecule.

The NH_2-terminal Domain of N-WASP Can Inhibit Binding of Arp2/3 Complex to the COOH-terminal VCA Segment

The VCA segment of N-WASP possesses two activities that are critical to its ability to activate actin nucleation. It binds to Arp2/3 complex through its CA region and to G-actin through its V region (Miki and Takenawa, 1998; Rohatgi et al., 1999). We tested if these interactions could be blocked by the NH_2-terminal WG fragment.

Whereas the VCA segment can bind to Arp2/3 complex with high affinity ($K_d \sim 100$ nM), the full-length, autoinhibited N-WASP molecule does not show detectable binding to Arp2/3 using pull-down assays (Fig. 2 B; Egile et al., 1999). To test the hypothesis that the low affinity of N-WASP for Arp2/3 complex is due to interactions between the NH_2-terminal domain and the VCA segment, we determined whether the WG and WGP fragments (Fig. 1 A) would compete with Arp2/3 for binding to VCA. The WG and WGP fragments were expressed as hexahistidine-tagged (HT) proteins using the baculovirus system in insect cells (Fig. 2 A). Both HT-WG and HT-WGP bound to GST-VCA in a dose-dependent manner and, more importantly, inhibited the interaction between Arp2/3 and GST-VCA (Fig. 2 C).

The HT-WG–GST-VCA complex was appropriately regulated by Cdc42 and $PI(4,5)P_2$. (Unless otherwise noted, Cdc42 refers to activated, GTPγS-loaded Cdc42, and $PI(4,5)P_2$ refers to synthetic liposomes containing 10:45:45 $PI(4,5)P_2$/PC/PI). The addition of Cdc42 or $PI(4,5)P_2$ to the HT-WG–GST-VCA complex stimulated the release of HT-WG from GST-VCA and the concomitant recovery of the GST-VCA–Arp2/3 interaction (Fig. 2 D). The ability of full-length N-WASP to bind to Arp2/3 could also be stimulated by Cdc42 and $PI(4,5)P_2$ (Fig. 2 E). Cdc42 and $PI(4,5)P_2$ produced the most potent increase in affinity when added together, explaining our previous observation that the ability of N-WASP to stimulate Arp2/3 complex is synergistically activated by these two regulators (Rohatgi et al., 1999). Because pull-down assays are only semiquantitative, we have not been able to determine whether the affinity of full-length, activated N-WASP for Arp2/3 is comparable to the high affinity (~100 nM) displayed by its isolated VCA segment.

The VCA segment of N-WASP has been shown to bind to G-actin (actin below its critical concentration for polymerization) through the V region that includes two verprolin homology segments (Miki and Takenawa, 1998). This actin binding site is separable from Arp2/3 site because the CA fragment, while sufficient to bind to Arp2/3 complex, does not bind to G-actin (Fig. 1 A and Fig. 3). The addition of saturating concentrations of the NH_2-terminal HT-WG and HT-WGP fragments (sufficient to completely block the interaction of GST-VCA with Arp2/3 complex) did not affect the interaction between GST-VCA and G-actin (Fig. 3). This is consistent with the ob-

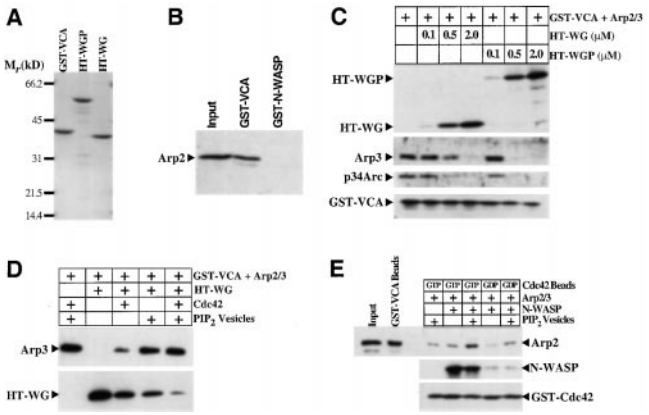

Figure 2. The NH_2-terminal domain of N-WASP inhibits binding of Arp2/3 complex to the COOH-terminal VCA segment in a Cdc42- and $PI(4,5)P_2$-regulated manner. (A) Purified protein preparations of the hexahistidine-tagged (HT) WG and WGP fragments and GST-VCA used in this study are shown on a 5–15% SDS–polyacrylamide gel. (B) Binding of GST-VCA or GST-fused full-length N-WASP (0.5 μM each) to Arp2/3 complex (0.1 μM) was assayed by incubating the components in solution and capturing the GST fusion protein on glutathione-Sepharose beads. The amount of Arp2/3 bound was determined by analyzing 50% of the input and 37.5% of the pulled down material on an α-Arp2 immunoblot. (C) Binding of GST-VCA (0.2 μM) to Arp2/3 (0.1 μM) was tested (as in B) in the presence of the indicated concentrations of HT-WG or HT-WGP. Immunoblotting was used to assay the amount of GST-VCA (α-GST), Arp2/3 (α-Arp3 and α-p34Arc), and HT-WG or HT-WGP (α-pentaHis) precipitated on the glutathione-Sepharose beads. (D) The ability of HT-WG (2 μM) to inhibit the binding of Arp2/3 (0.1 μM) to GST-VCA (0.2 μM) was tested in the presence of GTPγS-loaded Cdc42 (5 μM) or $PI(4,5)P_2$-containing vesicles (100 μM; $PI(4,5)P_2$/PI/PC = 10:45:45). (E) GST-Cdc42 beads, loaded with either GTPγS or GDP, were tested for their abilities to bind to Arp2/3 (1 μM) in the presence of N-WASP (1 μM) and $PI(4,5)P_2$-containing vesicles (100 μM). Arp2/3 pulled down by GST-Cdc42 beads in the absence of any N-WASP represents nonspecific, background binding under the conditions of the assay. For the α-Arp2 immunoblot, 7.5% of the input, 10% of the material pulled down on the GST-Cdc42 beads, and (as a control for comparison) 10% of the material pulled down by GST-VCA (1 μM) on glutathione- Sepharose beads was loaded on the gel.

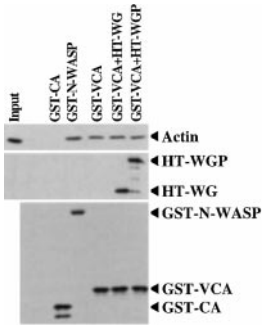

Figure 3. The NH_2-terminal domain of N-WASP does not inhibit binding of G-actin to the VCA segment. GST pull-down assays were used to measure the binding of actin (0.05 μM) to GST-CA, GST-N-WASP, GST-VCA (0.5 μM each), or to GST-VCA (0.5 μM) in the presence of HT-WG or HT-WGP (2.5 μM each). The amount of actin bound was compared using an α-actin immunoblot, loading 100% of the input and 40% of the pulled down material. The amounts of GST-N-WASP, GST-CA, GST-VCA, HT-WG, and HT-WGP pulled down were compared by immunoblotting with α-GST or α-pentaHis.

servation that the V region does not contribute to the binding interaction between GST-VCA and ^{35}S-labeled MT-WG (Fig. 1 D). Furthermore, a GST fusion of the full-length, autoinhibited N-WASP could bind to G-actin despite the presence of a putative intramolecular VCA–WG interaction (Fig. 3). These results are unexpected because the ability of full-length N-WASP to sequester G-actin and raise the critical concentration for polymerization has been shown to be much weaker than that of the isolated VCA fragment (Egile et al., 1999). Since our pull-down assays are only semiquantitative compared with critical concentration plots, one explanation for this difference is that we cannot detect modest (but functionally important) changes in the affinity for G-actin upon the binding of WG to VCA.

The NH_2-terminal Domain of N-WASP Can Inhibit the Actin Nucleation Activity of the COOH-terminal VCA Segment

Having established that the NH_2-terminal HT-WG fragment could inhibit the binding interaction between VCA and Arp2/3 in a Cdc42 and PI(4,5)P_2-regulated manner, we wanted to determine whether HT-WG could inhibit the ability of VCA to activate actin nucleation. We used an established fluorescence assay using pyrene-labeled actin to monitor the kinetics of actin assembly in the presence of GST-VCA, Arp2/3, and increasing concentrations of HT-WG (Cooper et al., 1983). HT-WG inhibited the ability of GST-VCA to accelerate actin polymerization in a dose-dependent manner (Fig. 4, A and B). Consistent with Arp2/3 binding data and the behavior of the full-length N-WASP molecule, the addition of GTPγS-Cdc42 or PI(4,5)P_2 relieved the inhibition of GST-VCA by HT-WG (Fig. 4, C and D). When added individually, Cdc42 and PI(4,5)P_2 had a much greater effect on the trans-inhibited WG–VCA complex than on full-length N-WASP. In the full-length molecule, the interaction between the WG and VCA segments likely occurs with a very high apparent affinity because of the fact that they are tethered together by the proline-rich region; thus, binding of both activators may be required to effectively disrupt this intramolecular interaction.

N-WASP Is a Monomer

Previously proposed models of N-WASP autoinhibition

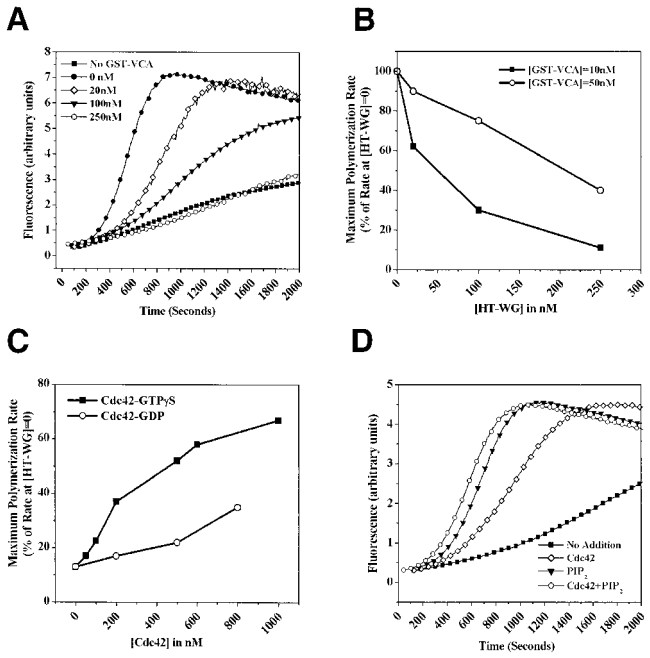

Figure 4. The NH_2-terminal domain of N-WASP inhibits Arp2/3-mediated actin nucleation activity of the VCA segment in a Cdc42, and PI(4,5)P_2-regulated manner. (A) The pyrene actin assay was used to monitor the polymerization of 1.3 μM G-actin (1 μM unlabeled actin + 0.3 μM pyrene labeled actin) in the presence of Arp2/3 (30 nM), GST-VCA (10 nM), and the indicated concentrations of HT-WG. (B) The ability of GST-VCA (10 nM or 50 nM) to activate Arp2/3 complex (30 nM) was measured in the presence of increasing concentrations of HT-WG. The maximum polymerization rate, calculated from the linear phase of polymerization curves of the type shown in A, is taken as a measure of Arp2/3 activation. (C) Cdc42-GTPγS can stimulate actin polymerization (1.3 μM actin, 30 nM Arp2/3) in the presence of GST-VCA (5 nM) and HT-WG (200 nM) more effectively than Cdc42-GDP. (D) The ability of either Cdc42-GTPγS (200 nM), PI(4,5)P_2-containing vesicles (10 μM), or both together to stimulate actin polymerization (1.3 μM actin, 30 nM Arp2/3 complex) in the presence of GST-VCA (5 nM) and HT-WG (200 nM).

have been arbitrarily drawn to suggest the presence of an intramolecular interaction between the NH_2- and COOH termini of the molecule (Rohatgi et al., 1999). The ability of the WG–VCA complex, even when lacking the intervening proline-rich tether, to recapitulate the behavior of the full-length N-WASP molecule highlights the possibility that N-WASP is actually a homodimer (or homomultimer) and that autoinhibitory interactions occur in trans between the NH_2- and COOH termini of two different molecules.

To characterize the physical state of N-WASP in solution, we produced untagged rat N-WASP in insect cells and purified the protein to homogeneity by sequential chromatography over heparin, anion exchange, and gel filtration columns (Fig. 5 A). Analysis of the protein by equilibrium ultracentrifugation at concentrations (up to 0.55 mg/ml or 10 μM) well above the estimated cellular concentrations (50 nM) revealed that it behaved as a single species with a molecular mass of 56, 826 ± 1,085 D, which is within 5% of the molecular mass predicted from the

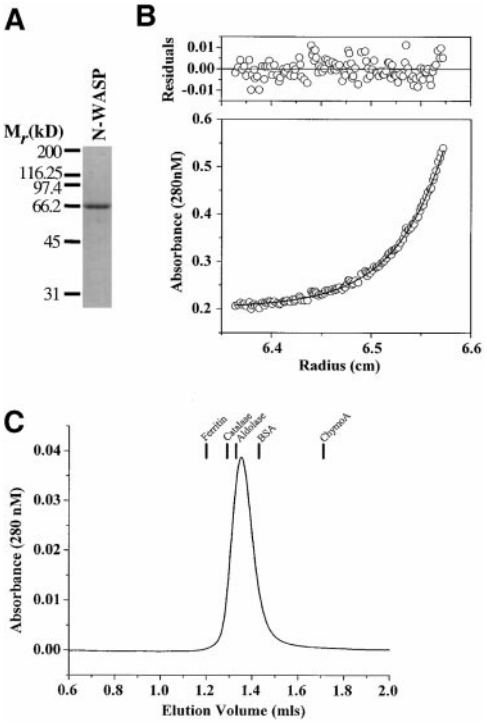

Figure 5. Hydrodynamic characterization of N-WASP. (A) A purified preparation of untagged rat N-WASP used for analytical ultracentrifugation and gel filtration chromatography is shown on a 10% SDS–polyacrylamide gel. (B) A radial absorbance plot showing the equilibrium distribution of N-WASP (0.55 mg/ml, 10 μM) after sedimentation in an analytical ultracentrifuge. The solid line indicates the best fit to the data, assuming a single component model, and the top panel shows residuals of the fit. (C) Elution profile from gel filtration chromatography of N-WASP on an analytical grade Superdex 200 column. The volumes at which various standard proteins elute are indicated.

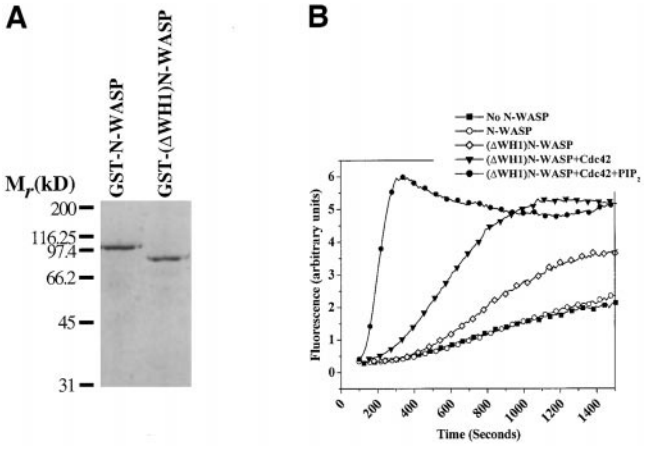

Figure 6. The WH1 domain is not required for the ability of $PI(4,5)P_2$ to activate N-WASP. (A) A 10% SDS–polyacrylamide gel showing purified protein preparations of GST-tagged wild-type N-WASP (GST-N-WASP) or a GST-tagged truncation mutant of N-WASP lacking the WH1 domain (GST-(ΔWH1) N-WASP). (B) Actin polymerization (1.3 μM actin, 30 nM Arp2/3 complex) in the presence of the indicated combinations of GST-N-WASP (50 nM), GST-(ΔWH1)N-WASP (50 nM), Cdc42-GTPγS (100 nM), or $PI(4,5)P_2$-containing vesicles (1 μM).

amino acid composition (54,324 D) (Fig. 5 B; Suzuki et al., 1998). To obtain an independent measure of the molecular mass, we determined the diffusion coefficient ($D_{20,w}$) of N-WASP by gel filtration chromatography and the sedimentation coefficient ($s_{20,w}$) by boundary sedimentation velocity ultracentrifugation (Fig. 5 C). The diffusion ($D_{20,w} = 4.87 \times 10^{-7}$ cm^2/s) and the sedimentation coefficients ($s_{20,w} = 3.16$S at 0.29 mg/ml or 5.4 μM) yield a molecular mass estimate of 55,147 D, which is within 2% of the predicted value.

The WH1 Domain Is Not Required for the Ability of $PI(4,5)P_2$ to Activate N-WASP

While Cdc42 interacts with N-WASP through the G-protein binding domain, the sequence elements in N-WASP that confer sensitivity to $PI(4,5)P_2$ have not been precisely mapped (Miki et al., 1998a). We have speculated that $PI(4,5)P_2$ activates N-WASP through its WH1 domain based on a report describing a binding interaction between $PI(4,5)P_2$ and a partial NH_2-terminal fragment of the WH1 domain (residues 1–127; Miki et al., 1996). We produced an N-WASP molecule lacking the WH1 domain as a GST fusion protein (GST-(ΔWH1)N-WASP; Fig. 6 A). The activation of this molecule by Cdc42 and $PI(4,5)P_2$ was compared with that of a GST fusion of wild-type N-WASP (GST-N-WASP). The GST tag does not change the behavior of wild-type N-WASP. As previously reported for untagged N-WASP, GST-N-WASP is partially activated by Cdc42 and fully activated in a synergistic fashion by Cdc42 and $PI(4,5)P_2$ (see Fig. 8 B). In the absence of Cdc42 and $PI(4,5)P_2$, the GST-(ΔWH1)N-WASP had a modestly higher basal Arp2/3 stimulation activity compared with the wild-type protein (Fig. 6 B). However, like the wild-type protein, the GST-(ΔWH1)N-WASP protein could be further activated by Cdc42 and maximally activated by a combination of Cdc42 and $PI(4,5)P_2$ (Fig. 6 B). While the WH1 domain may play an accessory role in stabilizing the autoinhibited conformation of N-WASP, a deletion of this domain clearly does not fully activate the molecule and, more importantly, does not abrogate its ability to respond to Cdc42 and $PI(4,5)P_2$.

The Basic Region (BR) Located Near the Cdc42 Binding Site Is Required for the Ability of $PI(4,5)P_2$ to Activate N-WASP

To find the sequence elements in N-WASP that mediate the effects of $PI(4,5)P_2$, we focused our attention on the GBR (residues 151–277) in the NH_2 terminus of N-WASP. There is a conserved BR (residues 186–196) in the GBR that is located just upstream of the consensus CRIB motif in N-WASP (Fig. 7 A). This BR is a good candidate for the site that binds to $PI(4,5)P_2$ because many motifs in proteins that interact with acidic phospholipids are basic in character, and the proximity of this BR to the Cdc42-binding CRIB motif may explain the synergistic effects of $PI(4,5)P_2$ and Cdc42 on N-WASP.

We used an established vesicle pull-down assay to determine whether the isolated GBR could bind to synthetic

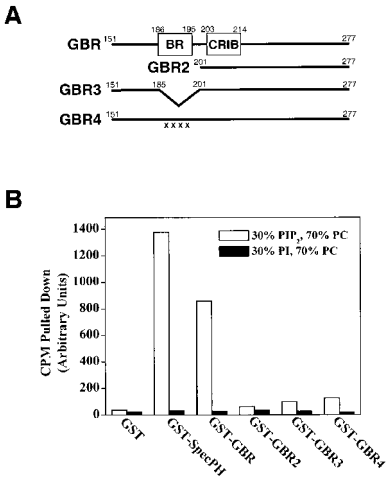

Figure 7. The BR in the NH_2 terminus of N-WASP specifically binds to $PI(4,5)P_2$. (A) Diagram showing various mutants of the GBR of bovine N-WASP, which includes the BR and the Cdc42/Rac interactive binding (CRIB) motif. In GBR4, the four Xs denote the substitution of four lysine residues (numbers 186, 189, 192, and 195) with glutamic acid residues. (B) Binding of the GST-GBR mutants shown in A to [^{3}H]phosphatidylcholine-labeled vesicles of the indicated compositions. A GST fusion of the β spectrin pleckstrin homology domain (GST-SpecPH) was used as a positive control in the assay.

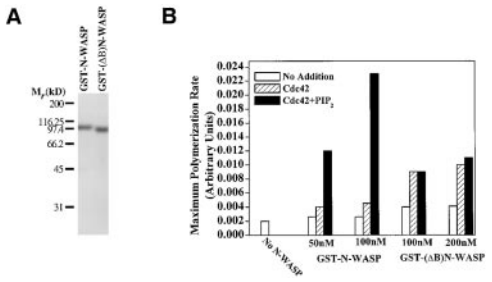

Figure 8. The BR in the NH_2 terminus is required for the ability of $PI(4,5)P_2$ to activate N-WASP. (A) A 10% SDS–polyacrylamide gel showing purified protein preparations of wild-type GST-N-WASP or a GST-tagged mutant of N-WASP containing an internal deletion of the BR (GST-(ΔB)N-WASP). (B) The maximum rate of polymerization was used to quantitate Arp2/3 activity (1.3 μM actin, 30 nM Arp2/3 complex) in the presence of two different concentrations of GST-N-WASP or GST-(ΔB) N-WASP and the indicated combinations of Cdc42-GTPγS (450 nM) and $PI(4,5)P_2$-containing vesicles. While the data shown in B is at 1 μM lipid, GST-(ΔB)N-WASP was $PI(4,5)P_2$-insensitive at higher lipid concentrations as well (up to 5 μM).

liposomes containing $PI(4,5)P_2$ (Rameh et al., 1997). A GST-GBR fusion protein was immobilized on glutathione-Sepharose beads and used to pull down vesicles labeled with trace amounts of [^{3}H]phosphatidylcholine. Compared with the GST control, GST-GBR bound to vesicles containing 30:70% $PI(4,5)P_2$/PC but not to vesicles containing 30:70% PI/PC (Fig. 7 B). This binding of GST-GBR to $PI(4,5)P_2$-containing vesicles could be disrupted by mutations in the basic region. An NH_2-terminal truncation of GBR (residues 201–276, GBR2), which deletes this basic region, eliminated binding to $PI(4,5)P_2$–containing vesicles (Fig. 7 B). Moreover, either an in-frame internal deletion of the basic stretch within GBR (Δ residues 186–200, GBR3) or a neutralization of positive charge (by the substitution of four of the lysine residues within this region with glutamic acid residues, GBR4) also eliminated binding (Fig. 7 B).

Since the vesicle binding data suggested that the BR within the GBR of N-WASP could mediate its interaction with $PI(4,5)P_2$, we proceeded to make a full-length GST-N-WASP fusion protein containing an in-frame deletion of this BR (Δ residues 186–195, GST-(ΔB)N-WASP; Fig. 8 A). It is important to note that this deletion does not remove the basic residues (e.g., K200) thought to be important for the interaction of N-WASP with Cdc42 (Abdul-Manan et al., 1999). We have verified that GST-(ΔB) N-WASP and wild-type GST-N-WASP bind to Cdc42 with similar affinities (data not shown). The GST-(ΔB)N-WASP protein was compared with the wild-type GST-N-WASP protein in its ability to activate Arp2/3-stimulated actin polymerization in response to Cdc42 or Cdc42 plus $PI(4,5)P_2$ vesicles (Fig. 8 B). GST-(ΔB)N-WASP modestly activated Arp2/3 on its own, and this basal activity could be stimulated by Cdc42. However, unlike the wild-type molecule, the activity of GST-(ΔB)N-WASP was completely insensitive to the further addition of $PI(4,5)P_2$. The BR seems to contribute to the stability of the autoinhibited conformation. When activated by saturating levels of Cdc42 alone, GST-(ΔB) N-WASP displayed twofold higher activity compared with its wild-type counterpart.

The Requirement for N-WASP in $PI(4,5)P_2$-stimulated Actin Polymerization in Xenopus Egg Extracts

The isolation of a $PI(4,5)P_2$-insensitive N-WASP molecule allowed us to dissect the role of N-WASP and of the N-WASP–$PI(4,5)P_2$ interaction in $PI(4,5)P_2$-stimulated actin polymerization in *Xenopus* egg extracts. Synthetic liposomes containing $PI(4,5)P_2$ stimulate actin polymerization in lipid-free HSS made from *Xenopus* egg extracts through a pathway that includes Cdc42 and Arp2/3 complex (Ma et al., 1998a). Since N-WASP is required for Cdc42-stimulated actin polymerization in *Xenopus* HSS, we tested whether it was also required for $PI(4,5)P_2$-stimulated actin assembly (Rohatgi et al., 1999). Using a polyclonal antibody described previously (Rohatgi et al., 1999), we immunodepleted >95% of the N-WASP from the HSS (Fig. 9 A). The depletion of N-WASP eliminated the ability of the HSS to support Cdc42-stimulated actin polymerization. The activity could be rescued by adding back purified, recombinant N-WASP protein (Fig. 9 B). Both untagged N-WASP and GST-tagged N-WASP could rescue the activity when added back to extracts depleted of endogenous N-WASP (Fig. 9, B and C).

To test the requirements for the WH1 domain and the BR of N-WASP in mediating $PI(4,5)P_2$-stimulated actin polymerization in the context of a more physiological extract system, we replaced endogenous N-WASP in *Xenopus* HSS with the GST-(ΔWH1)N-WASP and GST-

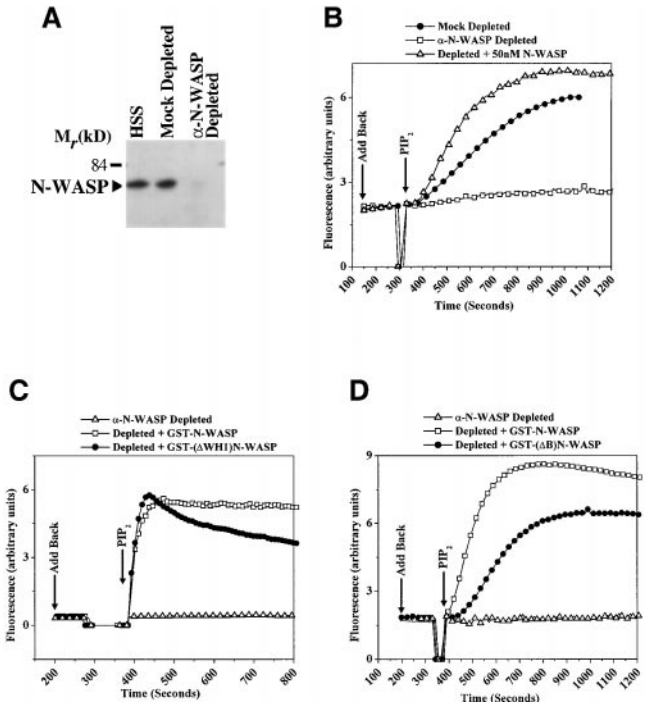

Figure 9. N-WASP is required for PI(4,5)P_2-stimulated actin polymerization in *Xenopus* HSS. (A) Affinity-purified α-N-WASP antibody or antibody buffer (mock) was used to immunodeplete N-WASP from *Xenopus* HSS, and the material in the supernatant was analyzed for the presence of N-WASP by immunoblotting using the same α-N-WASP antibody. (B) Comparison of actin assembly stimulated by 100 μM PI(4,5)P_2-containing vesicles in mock-depleted HSS, α-N-WASP–depleted HSS, and in depleted HSS reconstituted with 50 nM recombinant N-WASP. The add back of recombinant N-WASP to α-N-WASP–depleted extracts and the addition of PI(4,5)P_2-containing vesicles was performed at the time points indicated by the arrows. (C and D) The abilities of GST-N-WASP, GST-(ΔWH1)N-WASP, or GST-(ΔB)N-WASP (100 nM each) to restore PI(4,5)P_2-stimulated actin polymerization to HSS depleted of endogenous N-WASP.

(ΔB)N-WASP mutants described above. The mutant proteins, when added back to extracts depleted of endogenous N-WASP, did not stimulate spontaneous, signal-independent actin polymerization, confirming that they are substantially autoinhibited (Fig. 9, C and D). Based on both the initial rate of polymerization and the maximum amount of actin polymerized, the GST-(ΔWH1)N-WASP was just as effective as wild-type GST-N-WASP in restoring PI(4,5)P_2-stimulated actin assembly (Fig. 9 C). Interestingly, the actin polymerized in the GST-(ΔWH1) N-WASP–containing extract seemed to be less stable and partially depolymerized at later time points. The GST-(ΔB)N-WASP, which is PI(4,5)P_2-insensitive in the purified system, was also capable of restoring PI(4,5)P_2-stimulated actin assembly to HSS depleted of endogenous N-WASP (Fig. 9 D). However, compared with GST-N-WASP–containing extracts, the GST-(ΔB)N-WASP–containing extracts polymerized less total actin and did so with slower kinetics (characterized by a longer lag phase and a reduced initial rate of polymerization).

Discussion

Mechanism of N-WASP Inhibition and Activation

The physical interaction between the NH_2- and COOH termini of WASp family proteins has been used as the basis to propose a model in which this interaction locks the molecule in an autoinhibited state. We now show that an NH_2-terminal fragment of N-WASP, including the WH1 domain and the G-protein binding region, functions as a regulatory domain and inhibits, even in trans, actin nucleation by the COOH-terminal VCA segment by occluding Arp2/3 binding site. Activation of N-WASP by Cdc42 and PI(4,5)P_2 leads to two changes: (1) the affinity between the WG and VCA domains is reduced; and (2) the Arp2/3 binding site on VCA is exposed. The proline-rich segment of N-WASP appears to be dispensable both for the ability of the NH_2 terminus to inhibit the activity of the VCA segment and for the ability of Cdc42 and PI(4,5)P_2 to relieve this inhibition.

These results can be accommodated into either of two models for N-WASP activation that have been proposed in the literature (Fig. 10). In the first model (Model 1), the autoinhibitory interaction occurs in cis between the NH_2- and COOH termini of the same molecule (Miki et al., 1998a). In the second model (Model 2), N-WASP is a homodimer (or homomultimer) and the autoinhibitory WG–VCA interaction occurs in trans between two different molecules (Carlier et al., 2000). Recent structural studies on the p21 activated kinase, which like N-WASP switches between autoinhibited and Cdc42-bound conformations, demonstrated that the GBD region can serve as a dimer interface (Lei et al., 2000). Based on our finding that full-length, autoinhibited N-WASP is a monomer by both equilibrium and velocity ultracentrifugation at concentrations (>5 μM) well above cellular concentrations, we favor Model 1. In addition, GST-tagged N-WASP, which is forced into a dimeric form because of the GST moiety, behaves in a manner indistinguishable from the untagged protein in actin polymerization assays performed in the purified system or in extracts. Model 2 was proposed, in part, on the finding that a hexahistidine-tagged human N-WASP protein has a tendency to self-associate at concentrations above ~100 nM based on cross-linking data

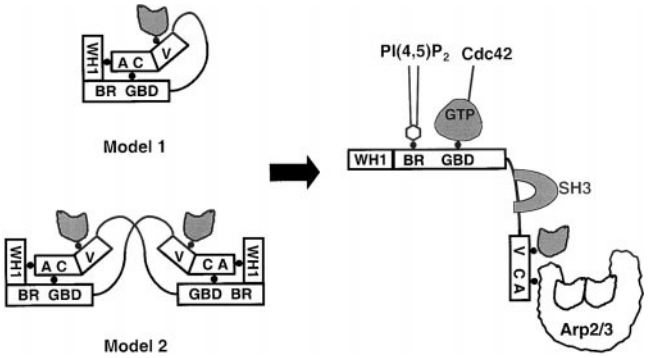

Figure 10. Two models for N-WASP activation. A black circle has been placed between sequence elements or proteins that have been shown to physically interact.

and on a reported $s_{20,w}$ of 5.45S (at 4 μM; Carlier et al., 2000). This is significantly higher than the $s_{20,w}$ value of 3.16S (at 5 μM) measured by us for untagged rat N-WASP. Since the human and rat proteins are ~95% identical, it is unlikely that this discrepancy in the $s_{20,w}$ value represents a species-specific difference. More likely, the hexahistidine tag or associated leader sequences might contribute to the tendency for the human protein to self-associate.

Sequence Elements that Mediate the PI(4,5)P_2 Effect

Contrary to our previous hypothesis, we have found that the WH1 domain does not mediate the effects of PI(4,5)P_2 on N-WASP. Instead, a BR located just upstream of the CRIB domain is required for the effects of PI(4,5)P_2 because a deletion of this segment generates an N-WASP molecule that is PI(4,5)P_2-insensitive in the purified assay system. This mutant molecule is not simply misfolded into an inactive state because it can activate Arp2/3 complex in a Cdc42-stimulated manner, and it can restore actin polymerization activity to *Xenopus* extracts depleted of endogenous N-WASP. The BR has been postulated to bind to the acidic region in the VCA domain through an electrostatic interaction (Miki et al., 1998a). However, an internal deletion of the BR does not significantly reduce the affinity of the NH_2-terminal WG region for GST-VCA (data not shown). Thus, PI(4,5)P_2 might work, not simply by interfering with an electrostatic BR–VCA interaction, but rather by destabilizing the fold adopted by the adjacent GBD region in the autoinhibited state. Alternatively, recruitment of N-WASP to the surface of PI(4,5)P_2 vesicles (via BR interactions) might indirectly destabilize the autoinhibited state by promoting multimerization. A BR is found in the NH_2 termini of all members of the WASp family, even in the Scar/WAVE proteins that lack a G-protein binding domain (Mullins, 2000). This sequence element may be an important regulatory site for the WASp family in general, mediating activation of these molecules by acidic phospholipids or other interacting proteins. It will be interesting to test whether IcsA and Grb2 can bind and activate the mutant N-WASP protein lacking the BR.

Recently, an NMR structure of the G-protein binding domain of human WASp (beginning at the CRIB motif but not including the basic region) artificially fused via a short linker to a fragment from the CA region has been solved (Kim et al., 2000). While this certainly represents the core of the autoinhibited fold of WASp (and likely N-WASP), our results suggest that the BR, which is just NH_2-terminal to the sequences included in WASp structure, can also function to mediate activation and, thus, probably influence the fold adopted by the GBD. The ability of the Grb2 Src homology domain 3 to activate N-WASP represents another example of a regulatory interaction that likely occurs outside this core fold defined by the NMR structure (Carlier et al., 2000). In this context, it will be important to define the sequence elements that mediate the activation of N-WASP by the *Shigella* protein IcsA. This property of sequence elements broadly distributed throughout N-WASP molecule to influence the stability of the autoinhibited fold is likely to be critical to its capacity to integrate and respond to a large set of signal inputs.

Dissecting a PI(4,5)P_2 Pathway in Xenopus Extracts

Phosphoinositides have been implicated as important regulators of actin assembly at a variety of different steps, including filament uncapping, severing, actin monomer binding as well as further upstream signaling roles. Because of the diverse effects of phosphoinositides on signaling proteins and actin binding proteins, it is often difficult to clearly trace lipid signaling pathways leading to actin assembly. We have previously shown that vesicles containing PI(4,5)P_2 can induce actin polymerization in *Xenopus* extracts in a Cdc42-dependent manner (Ma et al., 1998a). In turn, Cdc42-induced actin polymerization in extracts requires both N-WASP and Arp2/3 complex (Ma et al., 1998b; Rohatgi et al., 1999). Our demonstration that N-WASP is required for PI(4,5)P_2-stimulated actin assembly highlights the existence of a coherent signaling pathway in *Xenopus* extracts leading from PI(4,5)P_2 to de novo actin nucleation through Cdc42, N-WASP, and Arp2/3 complex. There is also evidence that this kind of pathway exists in somatic cells. Recently, PI(4,5)P_2 has been shown to mediate, through the WASp-Arp2/3 pathway, actin polymerization induced by sphingolipid cholesterol–rich membrane microdomains (Rozelle et al., 2000).

PI(4,5)P_2 can play two potential roles in this signaling pathway. First, it might indirectly stimulate the exchange of GTP for GDP on Cdc42 through the activation of an unidentified guanine nucleotide exchange factor (Ma et al., 1998a). Work in the purified system suggests that PI(4,5)P_2 also plays a role in directly activating N-WASP. Our identification of an N-WASP mutant (containing a deletion of the BR) that is PI(4,5)P_2-insensitive but Cdc42-sensitive in the purified system allowed us to dissect the relative contributions of these two potential functions of PI(4,5)P_2 in the *Xenopus* system. Since the (ΔB)N-WASP mutant is able to rescue PI(4,5)P_2-stimulated actin polymerization extracts depleted of endogenous N-WASP, we can conclude that the critical function of PI(4,5)P_2 is to activate Cdc42. This is consistent with the previous observation that Cdc42 alone can stimulate actin assembly in lipid-free *Xenopus* HSS (Ma et al., 1998a). Since Cdc42 is a relatively weak activator of N-WASP in the purified system, it is possible that another coactivator can substitute for PI(4,5)P_2 in extracts. In fact, biochemical fractionation of *Xenopus* and bovine brain extracts suggests that Cdc42-induced actin assembly requires a third factor in addition to N-WASP and Arp2/3 complex (Ma, L., R. Rohatgi, and M.W. Kirschner. 1999. American Society of Cell Biologist Annual Meeting. 2220 (Abstr.)). Identification of this unknown factor and elucidation of the pathway by which PI(4,5)P_2 activates Cdc42 are important future directions. For the PI(4,5)P_2-Cdc42-N-WASP-Arp2/3 pathway, the ability to complement experiments in complex extract or cellular systems with experiments in reconstituted, completely purified systems is a tremendous advantage that should continue to yield important insights into signal regulated actin assembly.

We thank Steve Harrison, Bruce Mayer, Maria-Carla Parrini, and Ming Lei for first raising the question of N-WASP dimerization and for helpful discussions; Ming Lei and Brian Baker for help with analytical ultracentrifugation; Lucia Rameh, Brian Duckworth and Lew Cantley for help with lipid binding assays; Nagi Ayad and Olaf Stemmann for carefully

reading the manuscript; Teresita Bernal and Louise Evans for help with baculovirus construction; Ethan Lee and Cathy Pfleger for expression vectors; and Tadaomi Takenawa, Hiroaki Miki, and Matt Welch for providing reagents. R. Rohatgi is a member of the Medical Scientist Training Program at Harvard Medical School.

This work was supported by a grant from the National Institutes of Health to M.W. Kirschner (GM26875).

Submitted: 14 June 2000
Revised: 21 July 2000
Accepted: 24 July 2000

References

Abdul-Manan, N., B. Aghazadeh, G.A. Liu, A. Majumdar, O. Ouerfelli, K.A. Siminovitch, and M.K. Rosen. 1999. Structure of Cdc42 in complex with the GTPase-binding domain of the 'Wiskott-Aldrich Syndrome' protein. *Nature*. 399:379–383.

Aspenstrom, P., U. Lindberg, and A. Hall. 1996. Two GTPases, Cdc42 and Rac, bind directly to a protein implicated in the immunodeficiency disorder Wiskott-Aldrich Syndrome. *Curr. Biol*. 6:70–75.

Banin, S., O. Truong, D.R. Katz, M.D. Waterfield, P.M. Brickell, and I. Gout. 1996. Wiskott-Aldrich syndrome protein (WASp) is a binding partner for c-Src family protein-tyrosine kinases. *Curr. Biol*. 6:981–988.

Bear, J.E., J.F. Rawls, and C.L. Saxe III. 1998. SCAR, a WASP-related protein, isolated as a suppressor of receptor defects in late *Dictyostelium* development. *J. Cell Biol*. 142:1325–1335.

Bi, E., and S.H. Zigmond. 1999. Actin polymerization: where the WASP stings. *Curr. Biol*. 9:R160–R163.

Carlier, M.F., P. Nioche, I. Broutin-L'Hermite, R. Boujemaa, C. Le Clainche, C. Egile, C. Garbay, A. Ducruix, P.J. Sansonetti, and D. Pantaloni. 2000. GRB2 links signalling to actin assembly by enhancing interaction of neural Wiskott-Aldrich Syndrome Protein (N-Wasp) with actin-related-protein (ARP2/3) complex. *J. Biol. Chem*. 275:21969–21974.

Cooper, J.A., S.B. Walker, and T.D. Pollard. 1983. Pyrene actin: documentation of the validity of a sensitive assay for actin polymerization. *J. Musc. Res. Cell Motil*. 4:253–262.

Derry, J.M., H.D. Ochs, and U. Francke. 1994. Isolation of a novel gene mutated in Wiskott-Aldrich syndrome. *Cell*. 79:922.

Egile, C., T.P. Loisel, V. Laurent, R. Li, D. Pantaloni, P.J. Sansonetti, and M.F. Carlier. 1999. Activation of the CDC42 effector N-WASP by the *Shigella flexneri* IcsA protein promotes actin nucleation by Arp2/3 complex and bacterial actin-based motility. *J. Cell Biol*. 146:1319–1332.

Hall, A. 1998. Rho GTPases and the actin cytoskeleton. *Science*. 279:509–514.

Kim, A.S., L.T. Kakalis, N. Abdul-Manan, G.A. Liu, and M.K. Rosen. 2000. Autoinhibition and activation mechanisms of the Wiskott-Aldrich syndrome protein. *Nature*. 404:151–158.

Kolluri, R., K.F. Tolias, C.L. Carpenter, F.S. Rosen, and T. Kirchhausen. 1996. Direct interaction of the Wiskott-Aldrich syndrome protein with the GTPase Cdc42. *Proc. Natl. Acad. Sci. USA*. 93:5615–5618.

Lei, M., W. Lu, W. Meng, M.C. Parrini, M.J. Eck, B.J. Mayer, and S.C. Harrison. 2000. Structure of PAK1 in an autoinhibited conformation reveals a multi-stage activation switch. *Cell*. 102:387–397.

Li, R. 1997. Bee1, a yeast protein with homology to Wiskott-Aldrich Syndrome protein, is critical for the assembly of cortical actin cytoskeleton. *J. Cell Biol*. 136:649–658.

Ma, L., L.C. Cantley, P.A. Janmey, and M.W. Kirschner. 1998a. Corequirement of specific phosphoinositides and small GTP-binding protein Cdc42 in inducing actin assembly in *Xenopus* egg extracts. *J. Cell Biol*. 140:1125–1136.

Ma, L., R. Rohatgi, and M.W. Kirschner. 1998b. The Arp2/3 complex mediates actin polymerization induced by the small GTP-binding protein Cdc42. *Proc. Natl. Acad. Sci. USA*. 95:15362–15367.

Machesky, L.M., and R.H. Insall. 1999. Signaling to actin dynamics. *J. Cell Biol*. 146:267–272.

Machesky, L.M., R.D. Mullins, H.N. Higgs, D.A. Kaiser, L. Blanchoin, R.C. May, M.E. Hall, and T.D. Pollard. 1999. Scar, a WASp-related protein, activates nucleation of actin filaments by the Arp2/3 complex. *Proc. Natl. Acad. Sci. USA*. 96:3739–3744.

Miki, H., and T. Takenawa. 1998. Direct binding of the verprolin-homology domain in N-WASP to actin is essential for cytoskeletal reorganization. *Biochem. Biophys. Res. Commun*. 243:73–78.

Miki, H., K. Miura, and T. Takenawa. 1996. N-WASP, a novel actin-depolymerizing protein, regulates the cortical cytoskeletal rearrangement in a PIP_2-dependent manner downstream of tyrosine kinases. *EMBO (Eur. Mol. Biol. Organ.) J*. 15:5326–5335.

Miki, H., T. Sasaki, Y. Takai, and T. Takenawa. 1998a. Induction of filopodium formation by a WASP-related actin-depolymerizing protein N-WASP. *Nature*. 391:93–96.

Miki, H., S. Suetsugu, and T. Takenawa. 1998b. WAVE, a novel WASP-family protein involved in actin reorganization induced by Rac. *EMBO (Eur. Mol. Biol. Organ.) J*. 17:6932–6941.

Mullins, R.D. 2000. How WASP-family proteins and the Arp2/3 complex convert intracellular signals into cytoskeletal structures. *Curr. Opin. Cell. Biol*. 12:91–96.

Mullins, R.D., J.A. Heuser, and T.D. Pollard. 1998. The interaction of Arp2/3 complex with actin: nucleation, high affinity pointed end capping, and formation of branching networks of filaments. *Proc. Natl. Acad. Sci. USA*. 95: 6181–6186.

Rameh, L.E., A.K. Arvidsson, K. Carraway, A.D. Couvillon, G. Rathbun, A. Crompton, B. VanRenterghem, M.P. Czech, K.S. Ravichandran, S.J. Burakoff, et al. 1997. A comparative analysis of the phosphoinositide binding specificity of pleckstrin homology domains. *J. Biol. Chem*. 272:22059–22066.

Ramesh, N., I.M. Anton, J.H. Hartwig, and R.S. Geha. 1997. WIP, a protein associated with Wiskott-Aldrich Syndrome protein, induces actin polymerization and redistribution in lymphoid cells. *Proc. Natl. Acad. Sci. USA*. 94: 14671–14676.

Rivero-Lezcano, O.M., A. Marcilla, J.H. Sameshima, and K.C. Robbins. 1995. Wiskott-Aldrich syndrome protein physically associates with Nck through Src homology 3 domains. *Mol. Cell. Biol*. 15:5725–5731.

Rohatgi, R., L. Ma, H. Miki, M. Lopez, T. Kirchhausen, T. Takenawa, and M.W. Kirschner. 1999. The interaction between N-WASP and the Arp2/3 complex links Cdc42-dependent signals to actin assembly. *Cell*. 97:221–231.

Rozelle, A.L., L.M. Machesky, M. Yamamoto, M.H. Driessens, R.H. Insall, M.G. Roth, K. Luby-Phelps, G. Marriott, A. Hall, and H.L. Yin. 2000. Phosphatidylinositol 4,5-bisphosphate induces actin-based movement of raft-enriched vesicles through WASP-Arp2/3. *Curr. Biol*. 10:311–320.

She, H.Y., S. Rockow, J. Tang, R. Nishimura, E.Y. Skolnik, M. Chen, B. Margolis, and W. Li. 1997. Wiskott-Aldrich syndrome protein is associated with the adapter protein Grb2 and the epidermal growth factor receptor in living cells. *Mol. Biol. Cell*. 8:1709–1721.

Suetsugu, S., H. Miki, and T. Takenawa. 1999. Identification of two human WAVE/SCAR homologues as general actin regulatory molecules which associate with the Arp2/3 complex. *Biochem. Biophys. Res. Commun*. 260:296–302.

Suzuki, T., H. Miki, T. Takenawa, and C. Sasakawa. 1998. Neural Wiskott-Aldrich syndrome protein is implicated in the actin-based motility of *Shigella flexneri*. *EMBO (Eur. Mol. Biol. Organ.) J*. 17:2767–2776.

Svitkina, T.M., and G.G. Borisy. 1999. Arp2/3 complex and actin depolymerizing factor/cofilin in dendritic organization and treadmilling of actin filament array in lamellipodia. *J. Cell Biol*. 145:1009–1026.

Symons, M., J.M. Derry, B. Karlak, S. Jiang, V. Lemahieu, F. Mccormick, U. Francke, and A. Abo. 1996. Wiskott-Aldrich syndrome protein, a novel effector for the GTPase CDC42Hs, is implicated in actin polymerization. *Cell*. 84:723–734.

Winter, D., T. Lechler, and R. Li. 1999. Activation of the yeast Arp2/3 complex by Bee1p, a WASP-family protein. *Curr. Biol*. 9:501–504.

Yarar, D., W. To, A. Abo, and M.D. Welch. 1999. The Wiskott-Aldrich syndrome protein directs actin-based motility by stimulating actin nucleation with the Arp2/3 complex. *Curr. Biol*. 9:555–558.